LA-UR-22-31516

Approved for public release; distribution is unlimited.

Title:	Aging and Lifetimes Program FY 2022 Annual Report - Part I: Update to BDNPA-BDNPF phase diagram
Author(s):	Edgar, Alexander Steven Goodwin, Lynne Alese Wong, Camille Hing Yang, Dali
Intended for:	Report
Issued:	2022-10-31

Aging and Lifetimes Program FY 2022 Annual Report
– Part I: Update to BDNPA-BDNPF phase diagram

Alex Edgar, Lynne Goodwin, Camille Wong, and Dali Yang (PI, dyang@lanl.gov)
MST-7: Engineered Materials, MST Division
Los Alamos National Laboratory, Los Alamos, New Mexico, USA 87545
October 05, 2022

Abstract

The eutectic mixture nitroplasticizer (NP) contains water, without exception, on the order of hundreds to thousands of parts per million depending on the exposure conditions. Therefore, to evaluate the properties of NP, one must consider that NP is not simply comprised of two constituents. Here we supplement previous work on the physical properties of NP (Edgar et al., 2020) by expanding on the experimental work therein and addressing inaccuracies detailed in a subsequent comment article (Brown, 2021). Specifically, the purpose of this work is to clarify and modify the phase diagram of the bis(2,2-dinitropropyl) acetal with bis(2,2-dinitropropyl) formal eutectic mixture by considering the effect of water concentrations on the nucleation process.

Introduction

In FY2022, work has been done to further define the eutectic phase diagram of bis(2,2-dinitropropyl) acetal with bis(2,2-dinitropropyl) formal (respectively called BDNPA and BDNPF [individually], or NP [mixed] herein). NP is a common nitroplasticizer used as softener in polymer bonded explosive binders. Although both BDNPA and BDNPF are solid at room temperature, some of their mixtures are liquid at room temperature, as illustrated in Figure 1. This observation indicates BDNPA with BDNPF exhibits melt point depression in the range of 35-65 wt% concentration of each component as reported in previous publications and reports on the material.[1, 2] The melt temperature was first reported as ranging from -15°C to +5°C by Milton Finger in 1972[1], and the construction of the eutectic phase diagram of BDNPA-BDNPF was then attempted in 1973 by T. Rivera[2]. However, the eutectic melt temperature has been reported as two widely differing values, i.e., -15°C[3, 4] and 14.5°C[2]. In 2020, we had attempted to resolve this large discrepancy in addition to reporting a wide range of physical properties of NP.[5] Our findings were criticized[6] for not providing validated experimental data to construct the phase diagram. Hence, the phase diagram reported in our previous paper (Edgar et al., 2020) is invalid because we mistakenly reported the melting points of NP without considering supercooling effect. To address these concerns, we have performed the work described here.

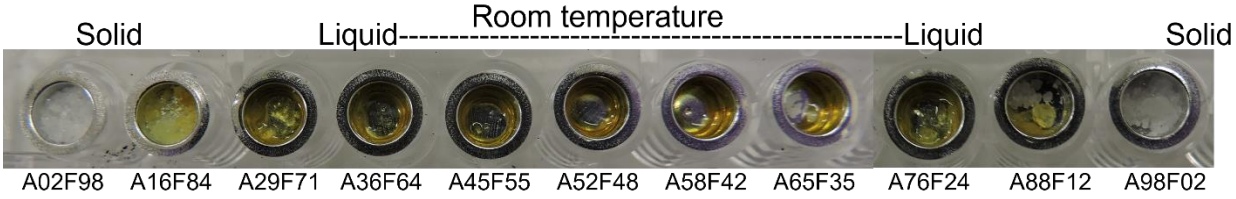

Figure 1: Various mass ratios of BDNPA and BDNPF imaged at room temperature, demonstrating melt point depression of the mixture ranging from 35-65% of each component.

It is important to consider NP contains an irremovable amount of water (~500 ppm at room temperature) without exception.[7] To further elaborate, in previous work, it has been shown that through HONO elimination, water is produced as a degradation product.[7-12]. Therefore, claiming NP is "dry" can only be applied relatively, and even if great lengths are taken to completely remove all water content from NP, water will be continually produced by the equilibrium 2 HONO ↔ H_2O + NO + NO_2.[13] When we attempted to construct the phase diagram of BDNPA and BDNPF mixture, our goal was to define the phase boundaries between their as manufactured eutectic mixture with variable water content, as shown in Figure 2.

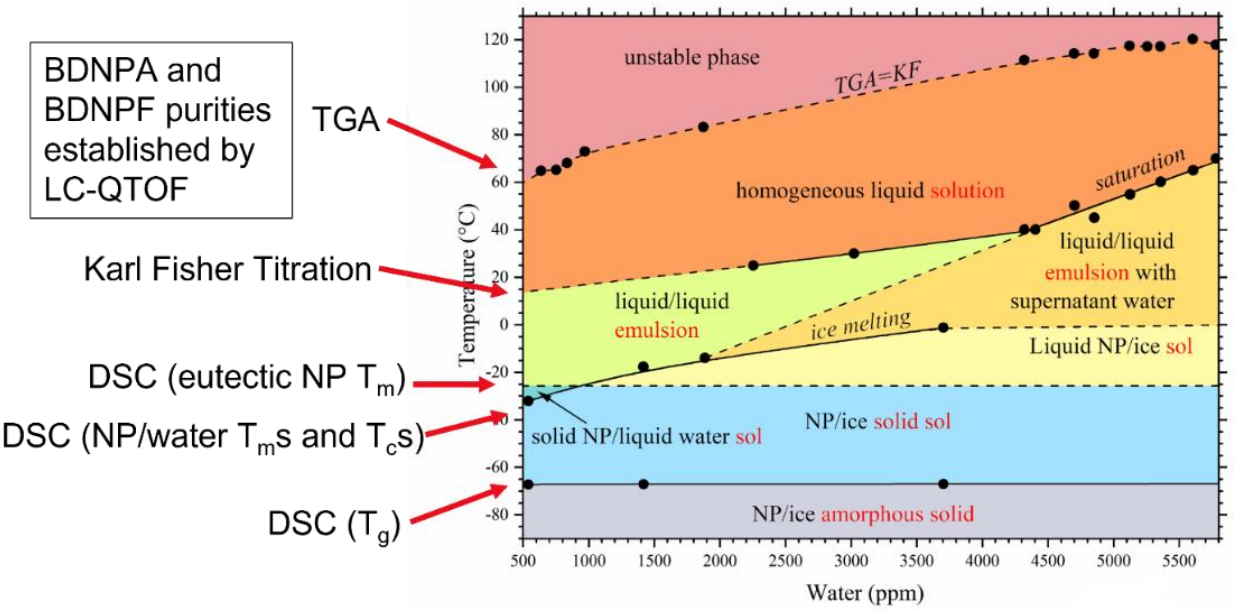

Figure 2: The NP-water phase diagram as previously published[5], the 'TGA=KF' line refers to the temperature where weight loss measurements collected by TGA are equal to water concentration values collected by KF, the line is dashed to display uncertainty as some of the weight loss may be due to other volatiles dissolved in the NP. The 'saturation' line refers to the boundary below which KF measurements became irreproducible due to phase separation as supernatant water. Indicated analysis techniques for each boundary shown left. Dashed lines indicate uncertainty associated with the results.

The eutectic NP T_m boundary was that reported in the large discrepancy (+15 vs. -15°C) as described above. Following the recommendation by the editor and reviewers of the Journal of Energetic Materials during the paper reviewing process, we ran differential scanning calorimetry (DSC) experiments and attempted to accurately define this value, as shown in Figure 3. The DSC signals in the middle concentration range mixtures show very weak trends, the phase diagram was constructed using signals which cannot be seen at the amplitude shown here and as such the work was criticized[6] accordingly. To compensate for the uncertainty in the DSC data, all points and lines indicate that uncertainty by being empty points or dashed respectively in the phase diagram on left.

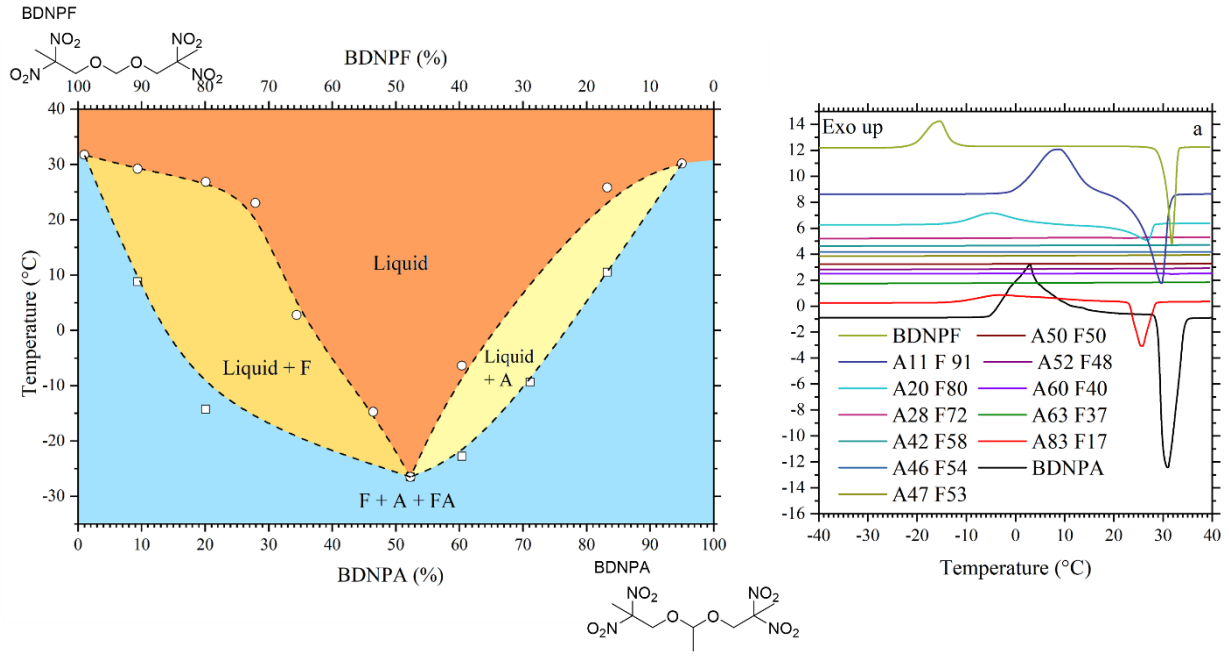

Figure 3: DSC determined eutectic phase diagram of BDNPA with BDNPF reported previously (left) and DSC heat flow thermograms (right). [4] Those signals for the middle concentration range of BDNPA/F mixtures show weak trends. Therefore, all points and lines indicate uncertainty by either being empty or dashed respectively in the phase diagram on left.

Experimental

Sample Preparation

Here a variety of NP component ratios were formulated, mixed, and tested to further clarify the thermal properties of these eutectic mixtures. The samples were evaluated by optical imaging at temperatures across the phase transition from liquid to solid and by DSC measurements with different heating rates. Samples were prepared according to the mixing ratios given in Table 1. Baseline NP and pure BDNPA(A)/BDNPF(F) were obtained from Pantex and used as received. The water concentration in the baseline NP is 600-800 ppm.[7] To explore the nucleation effect, several solid particles (tungsten carbide, hafnium dioxide, boron, boron nitride, poly(ether ether ketone) were added in baseline NP, detailed in Table 2, their thermal properties were evaluated using DSC measurements as well.

Table 1: Sample preparation information, "Solid_" samples have no premixed eutectic NP added.

Sample name	Short label	Total mass (mg)	Eutectic mixture (mg)	BDNPA (mg)	BDNPF (mg)	BDNPA (wt.%)	BDNPF (wt.%)
A02F98	**A1**	10.19	0	0	10.19	**2.29**	**97.71**
A16F84	**A2**	11.45	3.16	0	8.29	**15.95**	**84.05**
A29F71	**A3**	12.57	6.79	0	5.78	**29.03**	**70.97**
A36F64	**A4**	10.24	6.9	0	3.34	**35.65**	**64.35**
A45F55	**A5**	9.05	7.76	0	1.29	**44.74**	**55.26**
A52F48	**A6**	10.68	10.68	0	0	**51.80**	**48.2**
A58F42	**A7**	10.84	9.33	1.51	0	**58.21**	**41.79**
A65F35	**A8**	10.67	7.52	3.15	0	**65.38**	**34.62**
A76F24	**A9**	10.87	5.2	5.67	0	**75.79**	**24.21**
A88F12	**A10**	10.37	2.23	8.14	0	**87.91**	**12.09**
A98F02	**A11**	10.58	0	10.58	0	**97.80**	**2.20**
Solid_02A98F	**B1**	10.83	0	0	10.83	**2.30**	**97.70**
Solid_13A87F	**B2**	9.86	0	1.26	8.60	**14.49**	**85.51**
Solid_23A77F	**B3**	9.55	0	2.14	7.41	**23.68**	**76.32**
Solid_33A67F	**B4**	10.47	0	3.75	6.72	**36.47**	**63.53**
Solid_45A55F	**B5**	15.63	0	6.85	8.78	**44.74**	**55.26**
Solid_50A50F	**B6**	15.32	0	7.61	7.71	**51.80**	**48.20**
Solid_55A45F	**B7**	15.18	0	8.72	6.46	**58.21**	**41.79**
Solid_67A33F	**B8**	10.15	0	6.92	3.23	**67.34**	**32.66**
Solid_77A23F	**B9**	9.86	0	7.62	2.24	**76.03**	**23.97**
Solid_87A13F	**B10**	10.06	0	8.79	1.27	**85.66**	**14.34**
Solid_98A02F	**B11**	10.51	0	10.51	0	**97.70**	**2.30**

Table 2: Particle nucleation sample preparation information.

Total sample mass (mg)	Eutectic mixture (mg)	Particle type	density (g/mL)	Seed (mg)	Note
33.85	16.42	Tungsten carbide	15.63	1.8	(only four micro spheres)
26.36	16.27	Hafnium (IV) oxide	9.68	0.41	(only two micro spheres)
18.88	15.98	Boron	2.3	0.6	
17.66	15.34	Boron nitride	2.1	0.22	
17.4	15.57	Poly (ether ether ketone)	1.3	0.53	

Imaging Methodology

Samples were contained in Tzero pans (TA Instruments 901683.901) and organized in covered 96-well Microtiter Microplates (Thermo Fisher Scientific). Samples were organized such that there

were one to four samples per tray. There were four Eutectic samples, three middle A/F ratio concentration range samples, and one eutectic NP sample per tray. Each microtiter microplate of samples was covered with a lid and enclosed in a padded manila mailing envelope to minimize temperature changes in between imaging. Padded envelopes containing the sample trays were stored upright at the designated temperature in one of four laboratory refrigerators or freezers to cool the samples at either +5°C, +11°C, +22°C (Room temperature), -5°C, -15°C or -30°C. The period of cooling is controlled for more than 10-50 days to ensure sufficient cooling time, as in the 1973 T. Rivera work[2] the samples were not cooled in a slow controlled manner, samples were quenched in Rivera at -10°C and held at temperature for 3 days, in our work we allowed much longer soak time and cooled to much lower temperatures to ensure an average cooling rate of less than 1°C/day. Imaging dates are recorded in Table 3. Relative humidity and room temperature were monitored using the Fisherbrand Traceable Relative Humidity/Temperature meter. The room temperature storage relative humidity was between <=25-33% and room temperature was approximately 22°C during the few months of the testing period.

All images were collected using a Nikon SMZ18 Stereo Microscope equipped with a SHR Plan Apo 0.5x WD-71 objective and C-W 10xB/22 widefield adjustable eyepiece at a magnification of 2x manual zoom and oblique coherent contrast illumination. Imaging software used to capture sample images was the NIS-Elements D Ver5.20.00 (Build1423).

To maximize and maintain the longevity of the incubation temperature and minimize the distance traveled from the refrigerators and freezers to the imaging center, the microscope was centrally located. Additionally, each tray contained a minimum number of samples, between 1-4 samples, to reduce the time of each tray outside the refrigerators/freezers for imaging. Travel time (walking) in between the refrigerator and freezer locations and microscope was tracked which gives a general idea as to how long the samples were outside of the desired temperature and in-between imaging. The microtiter plate remained in the padded manila envelope for all transportation from refrigerators or freezers.

-5°C and -30°C freezers were located farthest from the imaging microscope. The periods of time outside the desired temperature zone are following:

- 77 seconds to walk from the freezers to the camera.
- 113 seconds to take four pictures.
- 173 seconds to repack the tray/walk down the hall/ put the tray back into the freezer.

The total amount of time the tray was out of the -5°C and -30°C freezers was 363 seconds.

+5°C, +11°C refrigerators, +22°C (room temperature) and the -15°C freezer were located closest to the imaging microscope. The periods of time outside the desired temperature zone are following:

- 30 seconds to walk from the refrigerator, freezer, or area in the lab to the microscope and take the picture.
- 45 seconds to repack the tray/walk/ put the tray back into the refrigerator/freezer.

The total amount of time the tray was out of the +5°C, +11°C refrigerators, +22°C (Room temperature) and the -15°C freezer was 75 seconds.

Table 3: Sample imaging information by date and temperature in °C. On 8/31/21, all samples made from mixing solids with baseline NP (A1-A11) were transferred into a total of 3 trays/lids with four samples per tray. On 8/20/21, most individual samples made from solids (B1-B4 and B8-B11) were transferred into their own trays for a total of 8 trays/lids with one sample per tray. On 8/20/21, samples B5-B7 were transferred to a shared tray making one tray containing 3 samples.

Sample preparation information				**Image date and temperature (°C)**							
Sample name	**Short label**	**BDNPA (wt.%)**	**BDNPF (wt.%)**	**8/20/21**	**8/24/21**	**8/30/21**	**8/31/21**	**9/10/21**	**10/4/21**	**10/21/21**	**11/8/21**
A02F98	**A1**	**2.29**	**97.71**	22	22		10	-5	-15	-5	6
A16F84	**A2**	**15.95**	**84.05**	22	22		10	-5	-15	-5	6
A29F71	**A3**	**29.03**	**70.97**	22	22		10	-5	-15	-5	6
A36F64	**A4**	**35.65**	**64.35**	22	22		10	-5	-15	-5	6
A45F55	**A5**	**44.74**	**55.26**	-30				11	5	6	
A52F48	**A6**	**51.80**	**48.20**	-30				11	5	6	
A58F42	**A7**	**58.21**	**41.79**	-30				11	5	6	
A65F35	**A8**	**65.38**	**34.62**	22	22		10	-5	-15	-5	6
A76F24	**A9**	**75.79**	**24.21**	22	22		10	-5	-15	-5	6
A88F12	**A10**	**87.91**	**12.09**	22	22		10	-5	-15	-5	6
A98F02	**A11**	**97.80**	**2.20**	22	22		10	-5	-15	-5	6
Solid_02A98F	**B1**	**2.30**	**97.70**			-30		-15	-5	-15	-15
Solid_13A87F	**B2**	**14.49**	**85.51**			-30		-15	-5	-15	-15
Solid_23A77F	**B3**	**23.68**	**76.32**			-30		-15	-5	-15	-15
Solid_33A67F	**B4**	**36.47**	**63.53**			-30		-15	-5	-15	-15
Solid_45A55F	**B5**	**44.74**	**55.26**			-30		-15	-5	-15	-15
Solid_50A50F	**B6**	**51.80**	**48.20**			-30		-15	-5	-15	-15
Solid_55A45F	**B7**	**58.21**	**41.79**			-30		-15	-5	-15	-15
Solid_67A33F	**B8**	**67.34**	**32.66**			-30		-15	-5	-15	-15
Solid_77A23F	**B9**	**76.03**	**23.97**			-30		-15	-5	-15	-15
Solid_87A13F	**B10**	**85.66**	**14.34**			-30		-15	-5	-15	-15
Solid_98A02F	**B11**	**97.70**	**2.30**			-30		-15	-5	-15	-15

DSC characterization

DSC heat flow experiments were conducted using TA instruments discovery series 2500 Differential Scanning Calorimeter. Samples were hermetically sealed in Al Tzero pans (TA Instruments 901683.901), a wide variety of heating rates were tested from 0.1°C/min up to 50°C/min, over a range from -90°C to 40°C. Comparative results are presented herein with the eutectic sample at multiple heating rates (1.0, 5.0, 10, and 20°C/min) and multiple samples run at 10°C/min which showed reproducible results that have signal peaks visible in the resultant plots.

Results and discussion

DSC results of select A/F mixtures, are shown in Figure 4. There is a clear trend with the changes in the concentration of A and F, the melt peak of the A/F mixture shifts, as pointed out on the plot. Although the minima of these signals are clear, the onset and offset of the melting event are difficult to define, negating the accuracy of plotting these data in a tammann style plot. Therefore, displaying the data as heat of fusion vs. concentration, suggested by Geoff Brown, has been omitted from this report.

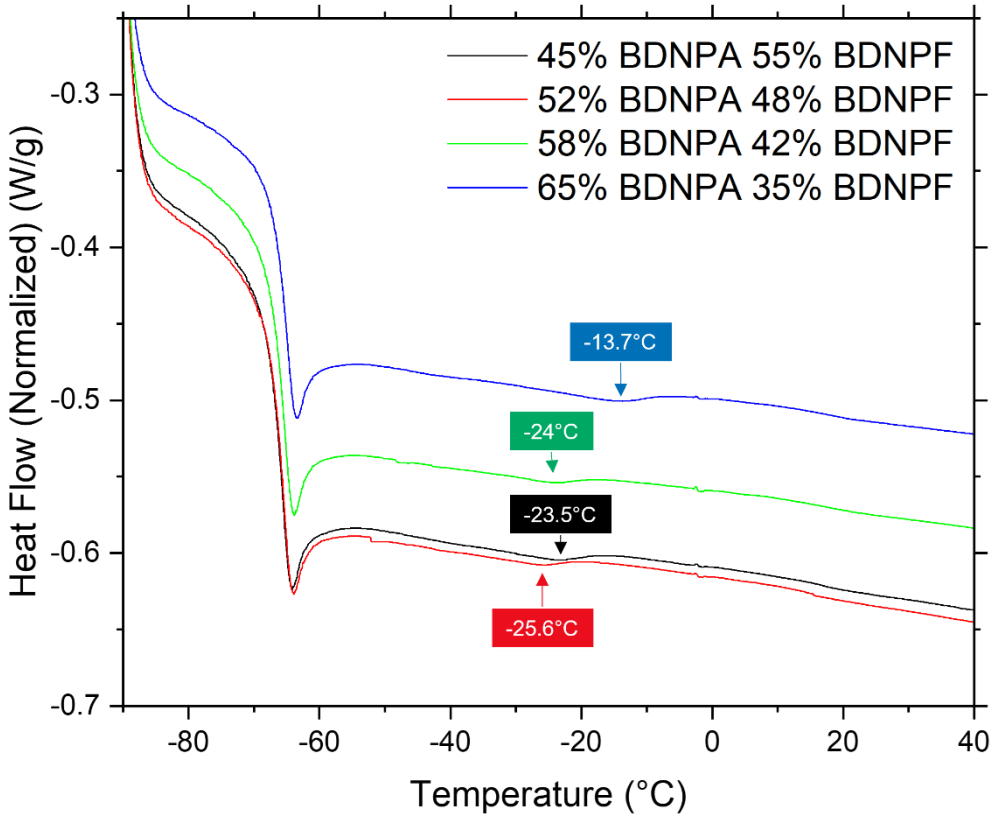

Figure 4: Exo up heat flow diagrams of near center values of mixed BDNPA and BDNPF with noted melt peak minima.

DSC results for a baseline NP as various heating rates are shown in Figure 5. The enthalpic relaxation peak clearly changes with heating rate, however the melt peak, indicated by the orange arrow, is both measurable and reproducible, remaining constant with changing heating rate, suggesting this peak is due to the melting behavior of eutectic NP.

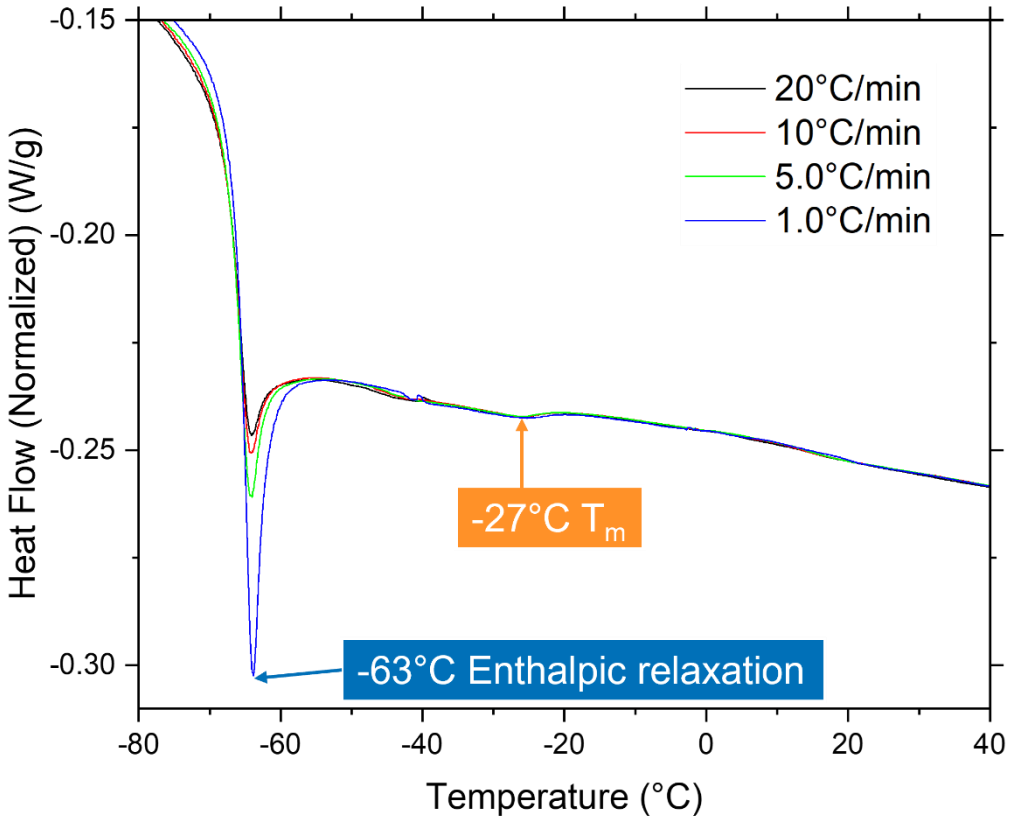

Figure 5: Exo up heat flow diagrams of eutectic NP at various heating ramp rates.

From Brown's comment paper, this peak, instead of assigning as the melting peak, was associated with the nucleation of water, which seemingly triggers the phase change as supercooling NP.[6] However, our interpretation is that since NP is invariably a three-component system BDNPA-BDNPF-water, the data presented in Figure 4 do help to define the eutectic melt temperature of this three-phase system around -27°C for baseline NP in this work, which agree with our previous finding.[5] Furthermore, to address questions about nucleation of solid phase in the eutectic material, several additional eutectic samples were made, and nucleation sources were deliberately introduced, as detailed above in Table 2, to test the validity of this hypothesis. From DSC measurements (data not shown here) and visual inspection, we observed no evidence of nucleation for the samples with various particles added. Rather we hypothesize the melting of NP can be nucleated by water molecules, and to reiterate, water presence is an inherent property in all NP. Indicating that the concentration of water may sway the behavior of NP in a more influential manner than the exact eutectic ratio of BDNPA to BDNPF.

The effect of water concentration on the melting point of NP-water mixtures, which can contain several thousand ppm of water, is given in our previous work.[5] The water concentration to apparent melt temperature relationship detailed therein can be described by Equation 1, expressing [H_2O] as ppm (wt/wt). The equation regression fits from DSC heat flow plotting from a variety of water concentrations in NP.

$$T_m(°C) = 16.059 * \ln([H_2O]) - 133.45,\ R^2 = 0.99847 \quad (1)$$

Assuming baseline NP has between 600 and 800 ppm water, the melt temperature calculates to -30.72 and -26.10°C respectively. The calculated result matches closely the observed value of approximately -27°C, back calculating the respective water concentration from the measured melt temp gives 756 ppm water. In previous work the water concentration in baseline NP was repeatedly measured as 780 ± 25 ppm on average by Coulometric Karl Fischer (KF) Titration[7], the back calculated value of 756 ppm falls just inside the error of the measurement demonstrating melt derived calculable water concentration matches the KF measured value reasonably well. The mixed samples were subject to a variable temperature program as described above. The resultant data collected by optical microscopy is shown in Figure 6.

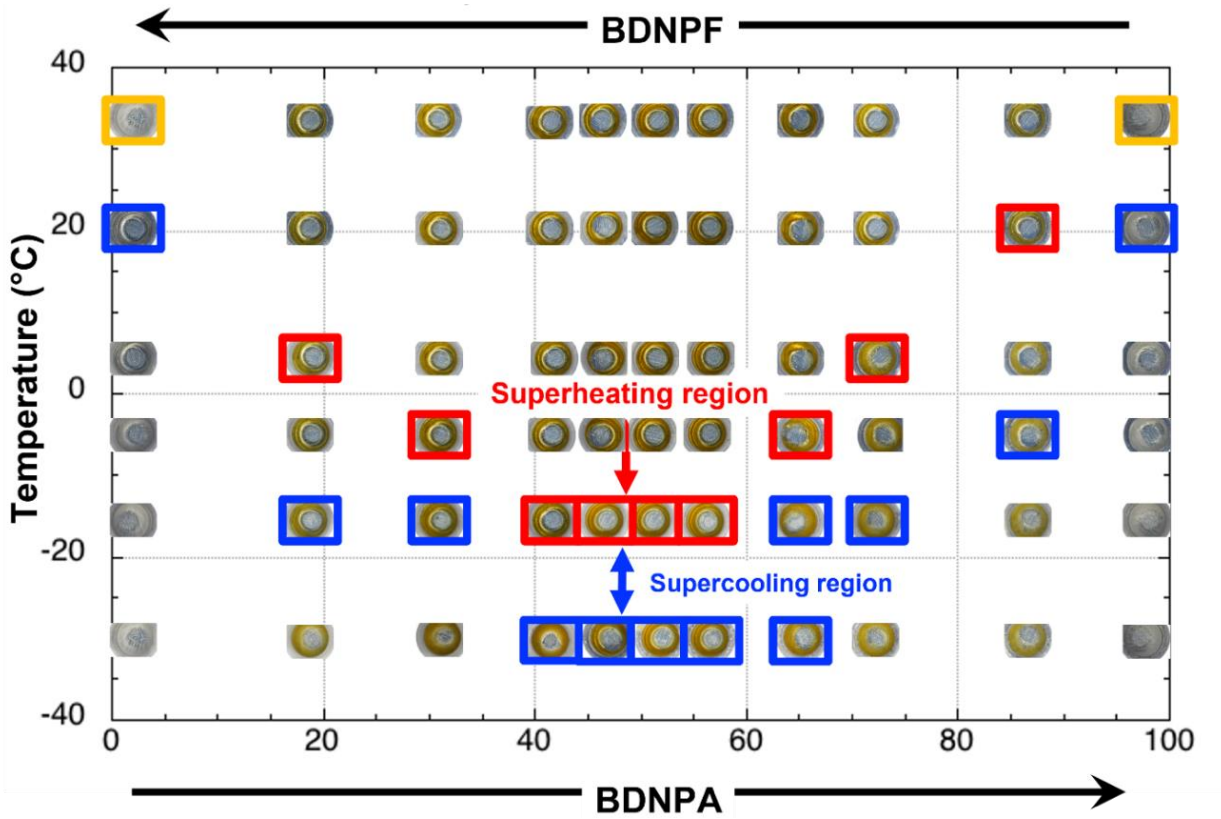

Figure 6: Optical microscope images of NP mixtures at various temperatures.

By visually observing the changes from solid to liquid and liquid to solid, we intend to demonstrate the observations made by practical use of the material, and revise boundaries of the phase diagram of A/F eutectic mixtures, as shown in Figure 7. Certainly, visual observation is convincing to those making the observation but can be deceiving without concrete metrological data to support. Therefore, we dash all lines derived from these observations and include the possibility that the solidification and melting of NP may be influenced by supercooling and superheating phenomena respectively, these phenomena were reported in 1972 by Milton Finger[1] and our results show similarity in shape to the phase diagram in that work, however shifted down by ~10-15°C at the center. We expect the differentiating factor in the results is a result of water content, closely tracked in our work but unknown in previous works.

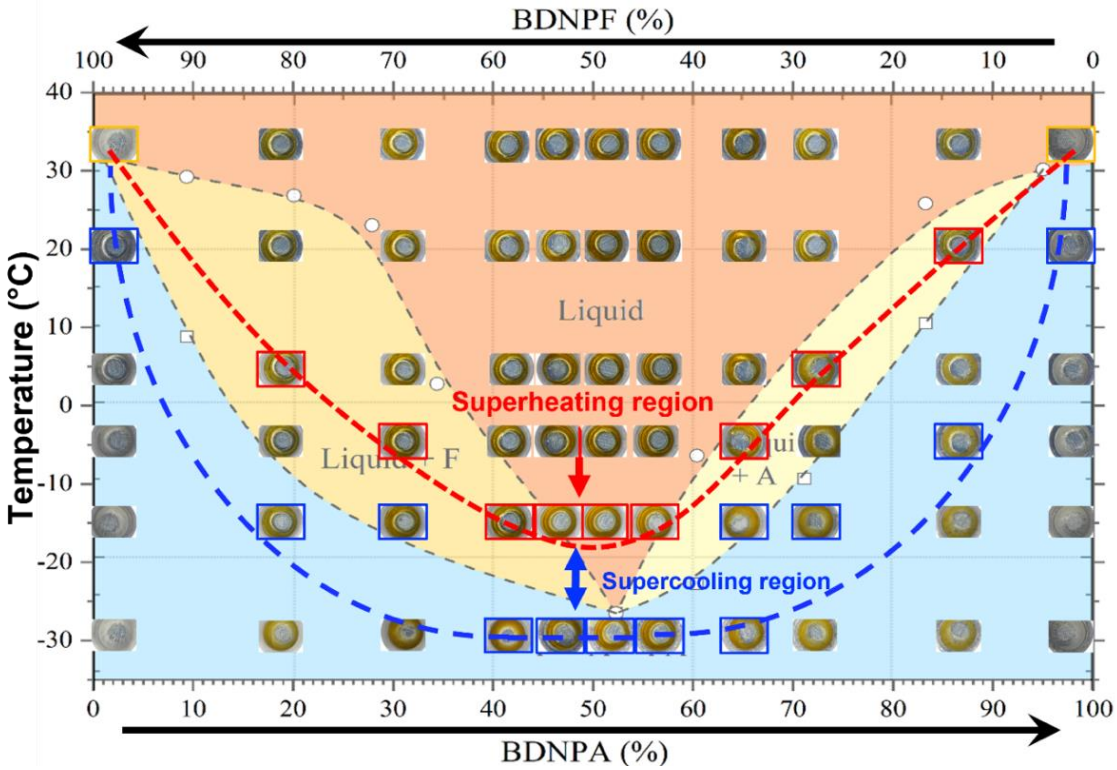

Figure 7: Optical microscope images of various NP mixtures overlaid on the previously published eutectic phase diagram.

Implementing observations of the supercooling and superheating phenomena, we apply changes to the NP-water phase diagram from our previous work. The original NP-water phase diagram is shown here as Figure 2, there the horizontal T_m line is derived from the measured T_m value -25.9°C. This event was originally considered to be a separate phase transition from the 'ice meting' line, complicating the diagram with three sol phases. In Figure 8, the revised NP-water phase diagram, reasoning that if water nucleates the solidification/melting of NP, we remove the assume T_m horizontal line. This change simplifies the diagram by reducing the assumptions made in its construction, resulting in a single sol phase. Furthermore, recognizing the "large tendency to supercool" indicated by Finger in 1972[1] and attempted to further clarification of the eutectic phase diagram by Rivera in 1973[2], we implement a region of superheating/supercooling, shown as blue hashed area. However, a distinction should be made between Figure 8 and previous works, we suggest that water plays a key role in the propagation of the superheating/supercooling phenomena associated with NP, whereas Finger lists NP as water insoluble and Rivera does not address water content.

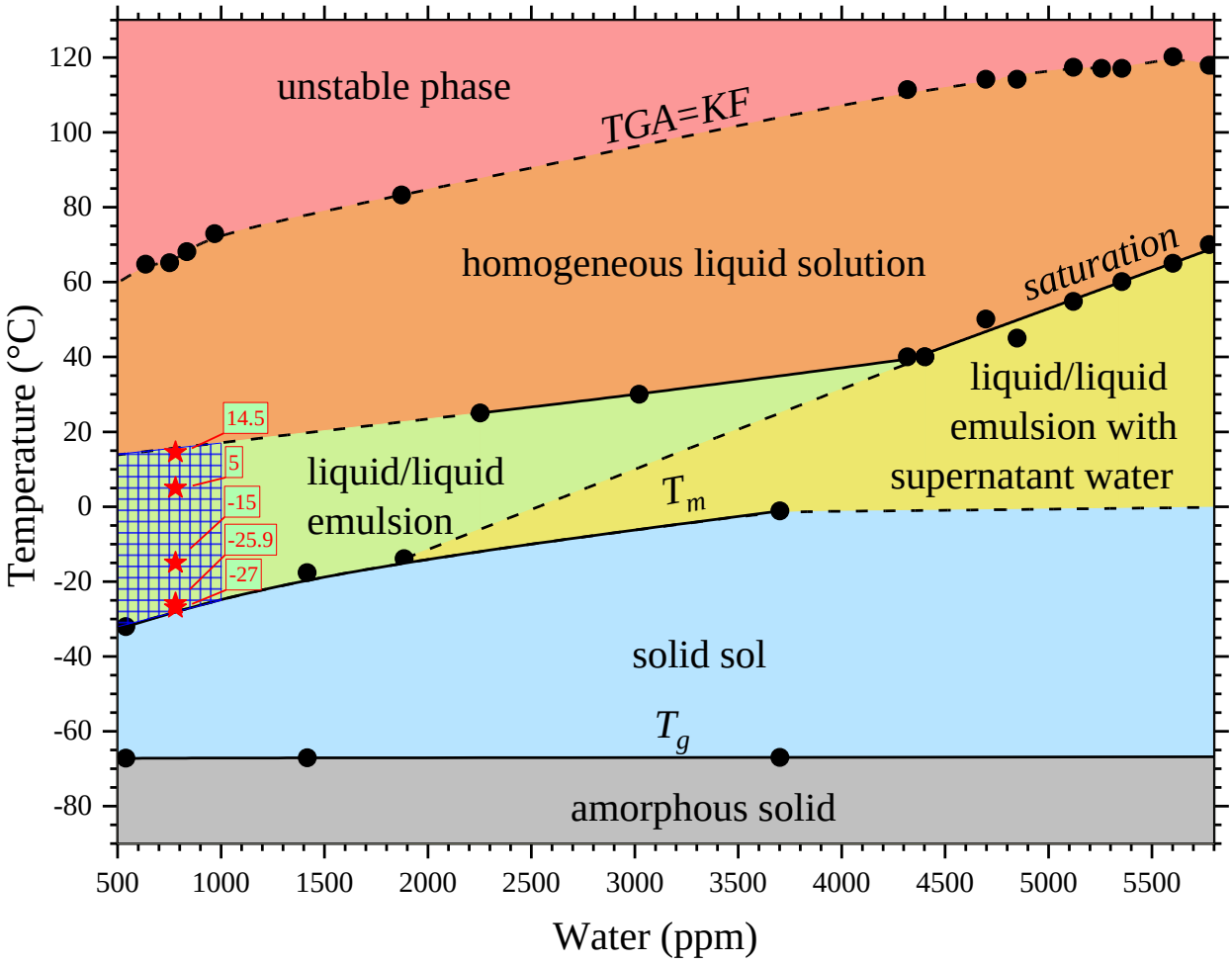

Figure 8: Updated NP-water phase diagram. Blue hashed area indicates region of suspected superheating and supercooling in reports and literature. Measured and literature values for change from solid to liquid are marked with red stars at -27°C from this work, -25.9°C from our previous work[5], -15°C and +5°C as range of supercooling from Finger[1] and later published as -15°C T_m by Shen[4] and Rauch[3], as T_m +15 from Rivera[2], in all cases water concentration was set to our measured value of 780 ppm, although the water content of previously collected data are not listed and therefore unknown.

In Figure 8 we plot all measured and literature values for changes from solid to liquid, marked with red stars at -27°C from this work, -25.9°C from our previous work[5], -15°C (solid below) and +5°C (liquid above) as range of supercooling from Finger[1] and later published as a T_m at -15°C by Shen[4] and Rauch[3], and as a eutectic T_m +14.5 from Rivera[2], in all cases water concentration was set to our measured value of 780 ppm. It is notable that all values fall within the liquid/liquid emulsion (green) region of the diagram. We suspect it possible that both Rivera and Finger may have had higher concentrations of water (likely up to ~2000 ppm) in their NP compared to those we measured based on the positions of the observed changes, however this is unclear, as the water concentration of their NP are unreported and therefore unknown. It is also imperative to point out that water induced superheating/supercooling region, as the blue hashed area in Figure 8, is bound at 1000 ppm water, this was placed arbitrarily and may extend to the full liquid region, furthermore

the dashed line between liquid/liquid emulsion and liquid/liquid emulsion with supernatant water regions (green and yellow respectively) is an extrapolation of the observed saturation line and may be influenced by superheating/supercooling as well.

Conclusion

Here we address concerns raised in our previously published work on the phase diagram determination of BDNPA with BDNPF. It is imperative to consider NP as not a two but three component system because BDNPA, BDNPF, and a trace amount of water (600-800 ppm at room temperature) are invariably present in practical use of the material (such as baseline NP), and its melting point may be due to the nucleation initiated by the irremovable amount of water molecules. Nevertheless, the uncertainty associated with superheating/supercooling of NP should be accounted for in the design of the phase diagrams. Hence, the NP-water phase diagram has been updated to remove previous assumptions, simplifying the diagram, and including a water induced superheating/supercooling field.

Acknowledgments

We would like to thank our Pantex colleagues Casey Huddleston and James Huskey for providing neat BDNPA/F samples. We also thank Geoff Brown at LANL for his consistent challenging of this and previous work. The work was funded by Aging and Lifetimes program.

References

(1) Finger, M. *Properties of Bis(2,2-dinitropropyl) Aectal and Bis(2,2-dinitropropyl) Formal, Eutectic Mixture*; UCID-16088; Lawrence Livermore National Laboratory, 1972.
(2) Rivera, T. *Study to determine the phase diagram of the BDNPA/F system*; LA-5313; Los Alamos Scientific Laboratory of the University of California, Los Alamos, NM, 1973.
(3) R. B. Rauch, R. B. Vapor Pressures, Mass Spectra and Thermal Decomposition Processes of Bis(2,2-Dintropropyl)acetal (BDNPA) and Bis(2,2-Dinitropropyl)formal *Propellants, Explos., Pyrotech.* **2007**, *32*, 97-116. DOI: https://doi.org/10.1002/prep.200700012.
(4) Shen, S. M., A. L. Leu, and H. C. Yeh. Thermal characteristics of polyurethane PEG and BDNPA F-Blends. *Thermochimica Acta* **1991**, *176* (75). DOI: https://doi.org/10.1016/0040-6031(91)80262-H.
(5) Edgar, A. S., J. Yang, M. Chavez, M. Yang, D. Yang. Physical Characterization of Bis(2,2-dinitropropyl) acetal and Bis(2,2-dinitropropyl) formal. *J. Energ. Mater.* **2020**, *38* (4), 483-503. DOI: https://doi.org/10.1080/07370652.2020.1737987.
(6) Brown, G. W. Comment on the paper "Physical characterization of Bis(2,2-dinitropropyl) acetal and Bis(2,2-dinitropropyl) formal" by Alexander Edgar, Justine Yang, Manuel Chavez, Michelle Yang & Dali Yang. *Journal of Energetic Materials* **2021**. DOI: https://doi.org/10.1080/07370652.2021.1942593.
(7) Yang, D., D. Z. Zhang. Role of Water in Degradation of Nitroplasticizer. *Poly. Degrad. Stab.* **2019**, *170* (109020). DOI: https://doi.org/10.1016/j.polymdegradstab.2019.109020.
(8) Yang, D., R. Pacheco, S. Edwards, K. R. Henderson, A. L. Wu, P. Stark. Thermal Stability of a Eutectic Mixture of Bis(2,2-dinitropropyl) acetal and formal: Part A. Degradation Mechanisms in Air and under Nitrogen Atmosphere, Degradation Mechanisms in Air and under Nitrogen Atmosphere. *Poly. Degrad. Stab.* **2016**, *129*, 380-398. DOI: https://doi.org/10.1016/j.polymdegradstab.2016.05.017.
(9) Yang, D., R. Pacheco, S. Edwards, J. Torres, K. Henderson, M. Sykora, P. Stark, S. Larson. Thermal Stability of a Eutectic Mixture of Bis(2,2-dintropropyl) acetal and formal: Part B. Degradation

Mechanisms under water and High Humidity Environments. *Poly. Degrad. Stab.* **2016**, *130*, 328-347. DOI: https://doi.org/10.1016/j.polymdegradstab.2016.06.007.
(10) Yang, D., A. S. Edgar, J. A. Torres, J. C. Adams, J. D. Kress. Thermal stability of a eutectic mixture of bis(2,2-dinitropropyl) acetal and formal: Part C. Kinetic compensation effect. *Propellants, Explos., Pyrotech* **2020**, *46* (1), 134-149. DOI: https://doi.org/10.1002/prep.202000042.
(11) Yang, D., A. Edgar, J. Torres, J. O'Neel, C. Wong. *FY2020 Annual Report of Aging and Lifetimes Program – Part II: Final Report of Four-Year Long Aging Experiment of Nitroplasticizer*; LA-CP-21-20217; Los Alamos National Laboratory, Los Alamos National Laboratory, 2020.
(12) Yang, D., A. S. Edgar, C. H. Wong, P. W. Peterson. *MST-7 research activities related to NP stability in the past 10 years*; LA-CP-21-20665; Los Alamos National Laboratory, 2021.
(13) D. K. Pauler, N. J. H., J. D. Kress. A mechanism for the decomposition of dinitropropyl compounds. *Phys. Chem. Chem. Phys.* **2007**, *9*, 5121-5126. DOI: https://doi.org/10.1039/B707604E.